ISSN: 2832-4293

Pan-American Journal of Mathematics 5 (2026), 17
https://doi.org/10.28919/cpr-pajm/5-17

MODELING BIOMASS-TRANSFER KLEPTOPARASITISM IN A PREDATOR-PREY SYSTEM WITH ACTIVE PREY DEFENSE

DEWI ANGGREINI[1,2], AGUS SURYANTO[1,*], ISNANI DARTI[1], WURYANSARI MUHARINI KUSUMAWINAHYU[1] AND M. ADIB JAUHARI DWI PUTRA[1]

ABSTRACT. This study proposes a three-dimensional predator-prey model incorporating a biomass-transfer formulation for kleptoparasitism and active prey antipredator behavior. The well-posedness of the system is established by confirming the existence, uniqueness, positivity, and boundedness of the solutions. Local and global stability analyses are performed to determine the analytical threshold conditions governing species persistence and extinction. Numerical simulations are subsequently conducted to verify the stability results and illustrate the system dynamics. The numerical observations indicate that a low kleptoparasitism intensity results in the extinction of the kleptoparasite due to insufficient energy gain. A moderate kleptoparasitism intensity permits stable coexistence but introduces bistability, making the long-term behavior dependent on initial population sizes. As the kleptoparasitism intensity increases further, the system loses its stable coexistence state and exhibits sustained population oscillations. At highly elevated kleptoparasitism intensity, the host predator population is significantly suppressed, which dampens the oscillations and allows the system to settle into a stable equilibrium. Numerical exploration of the parameter space suggests a trade-off between the interacting species: as prey defense strengthens, a higher stealing intensity is required for the kleptoparasite to survive, although the parameter region supporting stable coexistence remains narrow.

1. INTRODUCTION

Predator-prey models are an important topic in mathematical ecology. These systems help us understand how species coexist, how populations persist, and how ecosystems behave. Initially, the predator-prey model introduced by Lotka and Volterra [1,2] focused on a simple two-species system. However, real-world food webs are rarely that simple. Later, this simple two-species system was expanded to study the effects of various biological aspects such as harvesting [3,4], supplementary feeding [5,6], and others. Researchers also developed a one-prey-two-predator system to describe more complex realities. Over time, this multi-predator framework has become an important topic for analysis. There are phenomena of resource sharing, competitive exclusion, and complex interspecific interactions that occur when predators share food [7–9].

In systems with multiple predators, kleptoparasitism—the act of stealing resources already captured or processed by another organism—presents a compelling mechanism to study [10]. Instead of spending a

[1]DEPARTMENT OF MATHEMATICS, FACULTY OF SCIENCE, TECHNOLOGY, AND MATHEMATICS, UNIVERSITY OF BRAWIJAYA, MALANG, INDONESIA

[2]DEPARTMENT OF ELEMENTARY SCHOOL TEACHER EDUCATION, FACULTY OF TEACHER TRAINING AND EDUCATION, UNIVERSITAS SARJANAWIYATA TAMANSISWA, YOGYAKARTA, INDONESIA

Email address: anggreini1104@student.ub.ac.id, suryanto@ub.ac.id, isnanidarti@ub.ac.id, wmuharini@ub.ac.id, adibjauhari@student.ub.ac.id.

Submitted on Jun. 10, 2026.

2020 *Mathematics Subject Classification.* 92D25, 37G10, 34D20, 37N25.

Key words and phrases. predator–prey system; kleptoparasitism; antipredator behavior; global stability; Hopf bifurcation.

*Corresponding author.

lot of energy on hunting, kleptoparasites simply plunder the prey of other predators to optimize their own resource acquisition. Mechanistically, this food-kleptoparasitism behavior alters the energy transfer pathways within food webs and shifts the competitive relationships among consumers. This dynamic is closely tied to intraguild predation, where predators share a common prey while directly interacting through conflict [11]. Both field observations and mathematical models suggest that such plundering, alongside scavenging, can actually stabilize ecosystems by damping wild population oscillations [12]. These stabilizing effects and shifting competitive balances have naturally motivated the integration of kleptoparasitic interactions into modern predator–prey frameworks.

In addition to predator–predator interactions, prey species often respond to predation risk through behavioral adaptations. Such responses include increased vigilance, avoidance behavior, and defensive actions that reduce the probability of successful predation. Although these strategies may improve survival, they often involve ecological costs associated with reduced feeding opportunities or reproductive output. Wang et al. [13] demonstrated that fear-induced responses can significantly influence predator–prey dynamics even in the absence of direct predation. More generally, predator-induced non-consumptive effects have become an important topic in ecology because behavioral responses may affect population dynamics as strongly as direct consumption [14]. Recent studies have shown that fear effects and anti-predator behavior can alter stability properties, generate periodic oscillations, and induce bifurcation phenomena in predator–prey systems [15–19].

To capture these joint behaviors, several multi-species frameworks have recently been developed. For instance, Bhattacharjee et al. [20] modeled kleptoparasitism as a supplementary food source, though their work treats the prey population as entirely passive. Models using explicit nonlinear biomass-transfer equations provide a more direct description of the energy redistribution during food kleptoparasitism, but these frameworks overlook prey defensive behaviors entirely [21]. While Putri and Savitri [22] integrated both behaviors, their framework exhibits two distinct limitations. First, their model lacks an explicit biomass-transfer structure between the predators, meaning the host's energy loss is not directly coupled to the kleptoparasite's gain [22]. Second, they modeled anti-predator behavior as a defense mechanism between the competing predators themselves—specifically hyenas mobbing lions—leaving the primary prey population entirely passive [22]. A unified framework that couples active prey defense with explicit biomass-transfer kleptoparasitism remains completely unexplored.

To bridge these gaps, this paper introduces a new one-prey–two-predator model that couples explicit biomass-transfer kleptoparasitism with active prey defense. In our formulation, the mathematical representation of kleptoparasitism is inspired by the explicit biomass-transfer framework of Anggreini et al. [21], while the primary prey population employs active defenses that reduce the predation efficiency of both consumers. The main novelty lies in analyzing how the trade-off between this explicit predator kleptoparasitism and active prey evasion shapes long-term ecosystem stability. To evaluate this system, we first establish its mathematical well-posedness by proving the positivity and boundedness of solutions. We then determine all ecologically feasible equilibrium points and derive their local and global stability criteria. Finally, numerical simulations illustrate the dynamic transitions between species extinction, stable coexistence, and sustained oscillations under varying intensities of kleptoparasitism and defense.

2. Model Formulation

We build our model based on the explicit biomass-transfer kleptoparasitism framework proposed by Anggreini et al. [21], which extended the earlier kleptoparasitic system of Bhattacharjee et al. [20]. Unlike the indirect kleptoparasitism terms used by Bhattacharjee et al., the framework in [21] models kleptoparasitism as a direct biomass-transfer process. This structure gives a clear and mathematically consistent

representation of how energy moves between predator populations during food-kleptoparasitism interactions.

We expand this framework by allowing the prey population to actively defend itself against both predators. The prey does not act as a passive target; instead, it responds to predation risks through behavioral adaptations such as increased vigilance or collective evasion. These anti-predator responses directly lower the hunting efficiency of the consumers. Combining explicit biomass-transfer kleptoparasitism with active prey defense leads to the following non-linear differential equations:

$$\begin{aligned}
\frac{dx}{dt} &= r_1 x\left(1-\frac{x}{k}\right) - b_2 x y_1 - b_3 x y_2,\\
\frac{dy_1}{dt} &= b_2 c_4 x y_1 - a b_2 c_4 x y_1 y_2 - k_1 y_1 y_2 - d_2 y_1 - \eta_1 x y_1,\\
\frac{dy_2}{dt} &= b_3 c_5 x y_2 - k_2 y_1 y_2 - d_3 y_2 + c_6 x y_1 y_2 - \eta_2 x y_2.
\end{aligned} \tag{2.1}$$

System (2.1) describes the interaction among a prey population $x(t)$, a host predator population $y_1(t)$, and a kleptoparasitic predator population $y_2(t)$. The prey grows according to a logistic law characterized by the intrinsic growth rate r_1 and the environmental carrying capacity k. Both predators consume the same prey through Holling type-I predation terms.

The interaction between the predator populations consists of both competition and kleptoparasitism. The terms $k_1 y_1 y_2$ and $k_2 y_1 y_2$ represent interspecific competition, while the kleptoparasitic interaction is modeled through explicit biomass-transfer terms. Specifically, the quantity $a b_2 c_4 x y_1 y_2$ represents the biomass loss experienced by the host predator due to kleptoparasitism, whereas the term $c_6 x y_1 y_2$ represents the corresponding biomass gain of the kleptoparasitic predator. This formulation provides a direct description of resource redistribution between predator populations.

To account for prey defensive responses, anti-predator behavior is incorporated through the terms $\eta_1 x y_1$ and $\eta_2 x y_2$, which reduce the effective growth of both predator populations. Biologically, these terms represent the reduction in predation success caused by prey vigilance, avoidance behavior, or collective defense strategies. In addition, both predators experience natural mortality at rates d_2 and d_3, respectively. Therefore, the proposed model integrates prey defense mechanisms with explicit kleptoparasitic biomass transfer within a unified predator–prey framework.

All parameters in system (2.1) are assumed to be positive constant values. For clarity, their biological meanings are summarized in Table 1.

TABLE 1. Biological description of the model parameters

Parameter	Description
r_1	Intrinsic growth rate of the prey population
k	Environmental carrying capacity
b_2, b_3	Attack rates of the first and second predators on the prey
c_4, c_5	Conversion efficiency of prey biomass into predator biomass
c_6	Efficiency of biomass transfer via kleptoparasitism to the second predator
k_1, k_2	Interspecific competition coefficients between predators
d_2, d_3	Natural mortality rates of the host and kleptoparasitic predators
a	Kleptoparasitism intensity
η_1, η_2	Effectiveness of prey antipredator behavior against each predator

3. Preliminary Results

Before analyzing the dynamical behavior of system (2.1), we first verify that the model is mathematically and biologically well-posed. In particular, the existence, uniqueness, positivity, and boundedness of solutions ensure that all population variables remain biologically meaningful and finite over time.

3.1. **Existence and Uniqueness of Solutions.**

Theorem 3.1. *System* (2.1) *admits a unique global solution for every positive initial condition in* $\mathbb{R}^3_+$.

Proof. Since all nonlinear terms in system (2.1) are continuously differentiable in $\mathbb{R}^3_+$, the associated vector field is locally Lipschitz. Therefore, by the Picard–Lindelöf theorem, system (2.1) admits a unique local solution for every positive initial condition.

Furthermore, the positivity and boundedness results established below guarantee that the solution remains in a positively invariant bounded region. Hence, the solution exists globally for all $t \geq 0$. □

3.2. **Positivity and Boundedness.**

To ensure the biological feasibility of system (2.1), we show that all solutions remain nonnegative and bounded for all $t \geq 0$.

Theorem 3.2. *All solutions of system* (2.1) *with positive initial conditions remain positive for all* $t \geq 0$.

Proof. From system (2.1), we obtain

$$\frac{dx}{dt} = x\left(r_1\left(1-\frac{x}{k}\right) - b_2y_1 - b_3y_2\right),$$

which gives

$$x(t) = x(0)\exp\left(\int_0^t \left[r_1\left(1-\frac{x(s)}{k}\right) - b_2y_1(s) - b_3y_2(s)\right]ds\right) > 0.$$

Similarly,

$$y_1(t) > 0, \qquad y_2(t) > 0,$$

for all $t \geq 0$. Therefore, all solutions remain positive in $\mathbb{R}^3_+$. □

Theorem 3.3. *All solutions of system* (2.1) *are bounded in the region*

$$\Omega = \left\{(x, y_1, y_2) \in \mathbb{R}^3_+ : 0 \leq x + \frac{y_1}{c_4} + \frac{y_2}{c_5} \leq \frac{\rho}{\psi}\right\}.$$

Proof. Define

$$H(t) = x + \frac{y_1}{c_4} + \frac{y_2}{c_5}.$$

Differentiating $H(t)$ along the trajectories of system (2.1) yields

$$\begin{aligned}\frac{dH}{dt} =& r_1x\left(1-\frac{x}{k}\right) - \left(ab_2 - \frac{c_6}{c_5}\right)xy_1y_2 - \left(\frac{k_1}{c_4} + \frac{k_2}{c_5}\right)y_1y_2 \\ &- \frac{d_2}{c_4}y_1 - \frac{d_3}{c_5}y_2 - \frac{\eta_1}{c_4}xy_1 - \frac{\eta_2}{c_5}xy_2.\end{aligned}$$

Choose

$$\psi < \min\{d_2, d_3, \eta_1, \eta_2\},$$

and assume that

$$ab_2 > \frac{c_6}{c_5}.$$

Then,

$$\frac{dH}{dt} + \psi H \leq r_1x\left(1 - \frac{x}{k} + \frac{\psi}{r_1}\right).$$

Completing the square gives

$$\frac{dH}{dt} + \psi H \leq -\frac{r_1}{k}\left(x - \frac{(r_1+\psi)k}{2r_1}\right)^2 + \frac{(r_1+\psi)^2 k}{4r_1}.$$

Hence,

$$\frac{dH}{dt} + \psi H \leq \rho, \qquad \rho = \frac{(r_1+\psi)^2 k}{4r_1}.$$

By the comparison theorem,

$$H(t) \leq \frac{\rho}{\psi}(1 - e^{-\psi t}) + H(0)e^{-\psi t}.$$

Therefore,

$$0 < H(t) \leq \frac{\rho}{\psi},$$

which proves that all solutions of system (2.1) are bounded in Ω. □

4. Equilibrium Points and Stability Analysis

4.1. **Equilibrium Points.** The equilibrium points of system (2.1) are obtained from

$$\frac{dx}{dt} = \frac{dy_1}{dt} = \frac{dy_2}{dt} = 0.$$

The system admits the following equilibrium points:

(1) The trivial equilibrium $E_0 = (0, 0, 0)$, which represents the extinction of all populations.

(2) The predator-free equilibrium $E_1 = (k, 0, 0)$, which describes the persistence of the prey population in the absence of both predators.

(3) The first predator extinction equilibrium

$$E_2 = \left(\frac{d_3}{b_3c_5 - \eta_2}, 0, \frac{r_1(kb_3c_5 - \eta_2 k - d_3)}{b_3k(b_3c_5 - \eta_2)}\right),$$

which exists if

$$b_3c_5 > \eta_2, \qquad k > \frac{d_3}{b_3c_5 - \eta_2}.$$

(4) The second predator extinction equilibrium

$$E_3 = \left(\frac{d_2}{b_2c_4 - \eta_1}, \frac{r_1(kb_2c_4 - \eta_1 k - d_2)}{b_2k(b_2c_4 - \eta_1)}, 0\right),$$

which exists if

$$b_2c_4 > \eta_1, \qquad k > \frac{d_2}{b_2c_4 - \eta_1}.$$

(5) The coexistence equilibrium $E_4 = (x^*, y_1^*, y_2^*)$, where

$$x^* = \frac{k_1 y_2^* + d_2}{b_2c_4 - ab_2c_4y_2^* - \eta_1},$$
$$y_1^* = \frac{d_3(b_2c_4 - ab_2c_4y_2^* - \eta_1) - (b_3c_5 - \eta_2)(k_1y_2^* + d_2)}{c_6(k_1y_2^* + d_2) - k_2(b_2c_4 - ab_2c_4y_2^* - \eta_1)}.$$

The variable y_2^* is determined from the positive real root of a cubic polynomial equation derived from system (2.1). The detailed derivation is provided in Appendix A.

The coexistence equilibrium exists if

$$b_2c_4 > ab_2c_4y_2^* + \eta_1,$$
$$c_6(k_1y_2^* + d_2) > k_2(b_2c_4 - ab_2c_4y_2^* - \eta_1),$$
$$d_3(b_2c_4 - ab_2c_4y_2^* - \eta_1) > (b_3c_5 - \eta_2)(k_1y_2^* + d_2),$$
$$b_3c_5 > \eta_2.$$

4.2. **Local Stability Analysis.** The local stability of the equilibrium points is investigated using the linearization method. The Jacobian matrix of system (2.1) is

$$J = \begin{bmatrix} j_{11} & j_{12} & j_{13} \\ j_{21} & j_{22} & j_{23} \\ j_{31} & j_{32} & j_{33} \end{bmatrix},$$

where

$$\begin{aligned} j_{11} &= r_1 - \frac{2r_1 x}{k} - b_2 y_1 - b_3 y_2, \quad j_{12} = -b_2 x, \quad j_{13} = -b_3 x, \\ j_{21} &= b_2 c_4 y_1 - a b_2 c_4 y_1 y_2 - \eta_1 y_1, \quad j_{22} = b_2 c_4 x - a b_2 c_4 x y_2 - k_1 y_2 - d_2 - \eta_1 x, \\ j_{23} &= -a b_2 c_4 x y_1 - k_1 y_1, \quad j_{31} = b_3 c_5 y_2 + c_6 y_1 y_2 - \eta_2 y_2, \\ j_{32} &= -k_2 y_2 + c_6 x y_2, \quad j_{33} = b_3 c_5 x - k_2 y_1 - d_3 + c_6 x y_1 - \eta_2 x. \end{aligned}$$

The local stability of each equilibrium point is determined from the eigenvalues of the corresponding Jacobian matrix.

First, consider the trivial equilibrium $E_0 = (0, 0, 0)$. The Jacobian matrix at E_0 becomes

$$J(E_0) = \begin{bmatrix} r_1 & 0 & 0 \\ 0 & -d_2 & 0 \\ 0 & 0 & -d_3 \end{bmatrix}.$$

The eigenvalues of $J(E_0)$ are

$$\lambda_1 = r_1, \qquad \lambda_2 = -d_2, \qquad \lambda_3 = -d_3.$$

Since $r_1 > 0$, one eigenvalue is positive. Therefore, the trivial equilibrium E_0 is unstable. Biologically, this indicates that the prey population can recover from low density, preventing total extinction of the ecosystem.

Theorem 4.1. *The predator-free equilibrium $E_1 = (k, 0, 0)$ is locally asymptotically stable if*

$$k < \min\left\{ \frac{d_2}{b_2 c_4 - \eta_1}, \frac{d_3}{b_3 c_5 - \eta_2} \right\},$$

where

$$b_2 c_4 > \eta_1, \qquad b_3 c_5 > \eta_2.$$

Proof. Evaluating the Jacobian matrix at $E_1 = (k, 0, 0)$ gives

$$J(E_1) = \begin{bmatrix} -r_1 & -b_2 k & -b_3 k \\ 0 & b_2 c_4 k - d_2 - \eta_1 k & 0 \\ 0 & 0 & b_3 c_5 k - d_3 - \eta_2 k \end{bmatrix}.$$

Since $J(E_1)$ is upper triangular, its eigenvalues are

$$\lambda_1 = -r_1, \qquad \lambda_2 = b_2 c_4 k - d_2 - \eta_1 k, \qquad \lambda_3 = b_3 c_5 k - d_3 - \eta_2 k.$$

Since $r_1 > 0$, we have $\lambda_1 < 0$. Moreover,

$$\lambda_2 < 0 \iff k < \frac{d_2}{b_2 c_4 - \eta_1}, \qquad b_2 c_4 > \eta_1,$$

and

$$\lambda_3 < 0 \iff k < \frac{d_3}{b_3 c_5 - \eta_2}, \qquad b_3 c_5 > \eta_2.$$

Therefore, all eigenvalues have negative real parts whenever

$$k < \min\left\{ \frac{d_2}{b_2 c_4 - \eta_1}, \frac{d_3}{b_3 c_5 - \eta_2} \right\}.$$

Hence, E_1 is locally asymptotically stable. □

Biologically, the stability of E_1 indicates that both predators fail to invade the prey-only environment. This occurs when the prey carrying capacity is relatively small or when antipredator effects reduce the predation efficiency below the predator mortality thresholds.

Theorem 4.2. *The equilibrium point $E_2 = (x^*, 0, y_2^*)$, with*

$$x^* = \frac{d_3}{b_3c_5 - \eta_2}, \qquad y_2^* = \frac{r_1\left(k(b_3c_5 - \eta_2) - d_3\right)}{b_3k(b_3c_5 - \eta_2)},$$

is locally asymptotically stable if

$$b_2c_4x^* < ab_2c_4x^*y_2^* + k_1y_2^* + d_2 + \eta_1x^*,$$

and

$$b_3c_5 > \eta_2.$$

Proof. Evaluating the Jacobian matrix at $E_2 = (x^*, 0, y_2^*)$ gives

$$J(E_2) = \begin{bmatrix} -\frac{r_1x^*}{k} & -b_2x^* & -b_3x^* \\ 0 & b_2c_4x^* - ab_2c_4x^*y_2^* - k_1y_2^* - d_2 - \eta_1x^* & 0 \\ b_3c_5y_2^* - \eta_2y_2^* & -k_2y_2^* + c_6x^*y_2^* & 0 \end{bmatrix}.$$

One eigenvalue of $J(E_2)$ is

$$\lambda_1 = b_2c_4x^* - ab_2c_4x^*y_2^* - k_1y_2^* - d_2 - \eta_1x^*.$$

Thus,

$$\lambda_1 < 0 \iff b_2c_4x^* < ab_2c_4x^*y_2^* + k_1y_2^* + d_2 + \eta_1x^*.$$

The remaining eigenvalues are obtained from

$$J_1(E_2) = \begin{bmatrix} -\frac{r_1x^*}{k} & -b_3x^* \\ b_3c_5y_2^* - \eta_2y_2^* & 0 \end{bmatrix}.$$

By the Routh–Hurwitz criterion,

$$\operatorname{tr}(J_1(E_2)) = -\frac{r_1x^*}{k} < 0,$$

and

$$\det(J_1(E_2)) = b_3x^*y_2^*(b_3c_5 - \eta_2) > 0$$

whenever

$$b_3c_5 > \eta_2.$$

Hence, all eigenvalues have negative real parts under the stated conditions. Therefore, E_2 is locally asymptotically stable. □

The stability of E_2 implies that the second predator persists together with the prey population, while the first predator cannot invade the system. In this case, kleptoparasitic interactions and antipredator effects suppress the persistence of the first predator.

Theorem 4.3. *The equilibrium point $E_3 = (x^*, y_1^*, 0)$, with*

$$x^* = \frac{d_2}{b_2c_4 - \eta_1}, \qquad y_1^* = \frac{r_1(kb_2c_4 - \eta_1 k - d_2)}{b_2k(b_2c_4 - \eta_1)},$$

is locally asymptotically stable if

$$x^* < \frac{k_2y_1^* + d_3}{b_3c_5 + c_6y_1^* - \eta_2},$$

where

$$b_2c_4 > \eta_1, \qquad b_3c_5 + c_6y_1^* > \eta_2.$$

Proof. Evaluating the Jacobian matrix at $E_3 = (x^*, y_1^*, 0)$ gives

$$J(E_3) = \begin{bmatrix} -\dfrac{r_1x^*}{k} & -b_2x^* & -b_3x^* \\ b_2c_4y_1^* - \eta_1y_1^* & 0 & -ab_2c_4x^*y_1^* - k_1y_1^* \\ 0 & 0 & b_3c_5x^* - k_2y_1^* - d_3 + c_6x^*y_1^* - \eta_2x^* \end{bmatrix}.$$

One eigenvalue of $J(E_3)$ is

$$\lambda_1 = x^*(b_3c_5 + c_6y_1^* - \eta_2) - (k_2y_1^* + d_3).$$

Thus,

$$\lambda_1 < 0 \iff x^* < \frac{k_2y_1^* + d_3}{b_3c_5 + c_6y_1^* - \eta_2},$$

provided that

$$b_3c_5 + c_6y_1^* > \eta_2.$$

The remaining eigenvalues are obtained from

$$J_1(E_3) = \begin{bmatrix} -\dfrac{r_1x^*}{k} & -b_2x^* \\ b_2c_4y_1^* - \eta_1y_1^* & 0 \end{bmatrix}.$$

By the Routh–Hurwitz criterion,

$$\operatorname{tr}(J_1(E_3)) = -\frac{r_1x^*}{k} < 0,$$

and

$$\det(J_1(E_3)) = b_2x^*y_1^*(b_2c_4 - \eta_1) > 0$$

whenever

$$b_2c_4 > \eta_1.$$

Hence, all eigenvalues have negative real parts under the stated conditions. Therefore, E_3 is locally asymptotically stable. □

The equilibrium E_3 represents the persistence of the host predator together with the prey population, while the kleptoparasitic predator becomes extinct. This indicates that the host predator remains dominant when the kleptoparasitic gain is insufficient to overcome mortality and interspecific competition.

Theorem 4.4. *The coexistence equilibrium point $E_4 = (x^*, y_1^*, y_2^*)$ is locally asymptotically stable if the Routh–Hurwitz conditions*

$$\gamma_1 > 0, \qquad \gamma_3 > 0, \qquad \gamma_1\gamma_2 - \gamma_3 > 0$$

hold, where

$$\begin{aligned} \gamma_1 &= -K_{11}, \\ \gamma_2 &= -K_{23}K_{32} - K_{12}K_{21} - K_{13}K_{31}, \\ \gamma_3 &= K_{11}K_{23}K_{32} - K_{12}K_{23}K_{31} - K_{13}K_{21}K_{32}. \end{aligned}$$

Proof. Evaluating the Jacobian matrix at $E_4 = (x^*, y_1^*, y_2^*)$ gives

$$J(E_4) = \begin{bmatrix} K_{11} & K_{12} & K_{13} \\ K_{21} & K_{22} & K_{23} \\ K_{31} & K_{32} & K_{33} \end{bmatrix},$$

where

$$\begin{aligned} K_{11} &= -\frac{r_1 x^*}{k}, \quad K_{12} = -b_2 x^*, \quad K_{13} = -b_3 x^*, \\ K_{21} &= b_2 c_4 y_1^* - a b_2 c_4 y_1^* y_2^* - \eta_1 y_1^*, \quad K_{22} = 0, \\ K_{23} &= -a b_2 c_4 x^* y_1^* - k_1 y_1^*, \quad K_{31} = b_3 c_5 y_2^* + c_6 y_1^* y_2^* - \eta_2 y_2^*, \\ K_{32} &= -k_2 y_2^* + c_6 x^* y_2^*, \quad K_{33} = 0. \end{aligned}$$

The characteristic equation of $J(E_4)$ is

$$\lambda^3 + \gamma_1 \lambda^2 + \gamma_2 \lambda + \gamma_3 = 0.$$

By the Routh–Hurwitz criterion, all eigenvalues have negative real parts if

$$\gamma_1 > 0, \qquad \gamma_3 > 0, \qquad \gamma_1 \gamma_2 - \gamma_3 > 0.$$

Therefore, E_4 is locally asymptotically stable under the stated conditions.

Since the explicit form of $\gamma_1\gamma_2 - \gamma_3$ is highly complicated, the stability of E_4 is further explored numerically in Section 6. □

Overall, the local stability conditions show that predator persistence strongly depends on the balance between predation efficiency, antipredator effects, interspecific competition, and kleptoparasitic interactions. Variations in these parameters may drive transitions between extinction and coexistence states, leading to more complex dynamical behavior.

5. Global Stability Analysis

Local stability analysis only describes the behavior of the system near an equilibrium point. To investigate the long-term dynamics of system (2.1), we now analyze the global stability of the equilibria using the Lyapunov direct method and LaSalle's invariance principle.

Theorem 5.1. *The predator-free equilibrium $E_1 = (k, 0, 0)$ is globally asymptotically stable if*

$$k < \min\left\{ \frac{d_2}{b_2(1+c_4)}, \frac{d_3}{b_3(1+c_5)}, \frac{k_1+k_2}{c_6} \right\}.$$

Proof. Consider the Lyapunov function

$$V_1(x, y_1, y_2) = x - k - k \ln \frac{x}{k} + y_1 + y_2,$$

which is positive definite for $x > 0$.

Differentiating V_1 along the trajectories of system (2.1) gives

$$\frac{dV_1}{dt} = \left(\frac{x-k}{x} \right) \frac{dx}{dt} + \frac{dy_1}{dt} + \frac{dy_2}{dt}.$$

Substituting system (2.1) and simplifying (see Appendix B) yields

$$\frac{dV_1}{dt} \leq [k b_2(1+c_4) - d_2]\, y_1 + [k b_3(1+c_5) - d_3]\, y_2 + [c_6 k - k_1 - k_2]\, y_1 y_2.$$

Hence,

$$\frac{dV_1}{dt} < 0$$

provided that

$$k < \frac{d_2}{b_2(1+c_4)}, \qquad k < \frac{d_3}{b_3(1+c_5)}, \qquad k < \frac{k_1+k_2}{c_6}.$$

Moreover,

$$\frac{dV_1}{dt} = 0$$

if and only if

$$(x, y_1, y_2) = (k, 0, 0).$$

Therefore, by LaSalle's invariance principle, the equilibrium point $E_1 = (k, 0, 0)$ is globally asymptotically stable. □

Biologically, these conditions indicate that predator extinction occurs when predation efficiency and kleptoparasitic gain are insufficient to overcome mortality and interspecific competition. Strong kleptoparasitic interactions may further destabilize predator persistence by intensifying competition between the two predator populations.

Theorem 5.2. *The equilibrium point $E_2 = (x^*, 0, y_2^*)$ is globally asymptotically stable if*

$$b_2x^* + \alpha k_2 y_2^* < \frac{d_2}{c_4},$$

and

$$\alpha c_6 k < \frac{k_1}{c_4} + \alpha k_2,$$

where

$$\alpha = \frac{b_3}{b_3c_5 - \eta_2} > 0.$$

Proof. Consider the Lyapunov function

$$V_2(x, y_1, y_2) = x - x^* - x^* \ln \frac{x}{x^*} + \frac{1}{c_4}y_1 + \alpha \left(y_2 - y_2^* - y_2^* \ln \frac{y_2}{y_2^*} \right),$$

which is positive definite for $x, y_2 > 0$.

Differentiating V_2 along the trajectories of system (2.1) gives

$$\frac{dV_2}{dt} = \left(\frac{x - x^*}{x} \right) \frac{dx}{dt} + \frac{1}{c_4} \frac{dy_1}{dt} + \alpha \left(\frac{y_2 - y_2^*}{y_2} \right) \frac{dy_2}{dt}.$$

Using the equilibrium conditions at $E_2 = (x^*, 0, y_2^*)$ and simplifying (see Appendix C), we obtain

$$\frac{dV_2}{dt} \leq \left(b_2x^* + \alpha k_2 y_2^* - \frac{d_2}{c_4} \right) y_1 + \left(\alpha c_6 k - \frac{k_1}{c_4} - \alpha k_2 \right) y_1 y_2.$$

Hence,

$$\frac{dV_2}{dt} < 0$$

provided that

$$b_2x^* + \alpha k_2 y_2^* < \frac{d_2}{c_4},$$

and

$$\alpha c_6 k < \frac{k_1}{c_4} + \alpha k_2.$$

Moreover,

$$\frac{dV_2}{dt} = 0$$

if and only if

$$(x, y_1, y_2) = (x^*, 0, y_2^*).$$

Therefore, by LaSalle's invariance principle, the equilibrium point $E_2 = (x^*, 0, y_2^*)$ is globally asymptotically stable. □

Biologically, these conditions indicate that the second predator persists together with the prey population when mortality, competition, and antipredator effects suppress the invasion of the first predator population.

Theorem 5.3. *The equilibrium point $E_3 = (x^*, y_1^*, 0)$ is globally asymptotically stable if*

$$b_3x^* + \alpha a b_2 c_4 k y_1^* + \alpha k_1 y_1^* < \frac{d_3}{c_5},$$

and

$$\frac{c_6}{c_5}k < \alpha k_1 + \frac{k_2}{c_5},$$

where

$$\alpha = \frac{b_2}{b_2c_4 - \eta_1} > 0.$$

Proof. Consider the Lyapunov function

$$V_3(x, y_1, y_2) = x - x^* - x^* \ln \frac{x}{x^*} + \alpha \left(y_1 - y_1^* - y_1^* \ln \frac{y_1}{y_1^*} \right) + \frac{1}{c_5} y_2,$$

which is positive definite for $x, y_1 > 0$.

Differentiating V_3 along the trajectories of system (2.1) gives

$$\frac{dV_3}{dt} = \left(\frac{x - x^*}{x} \right) \frac{dx}{dt} + \alpha \left(\frac{y_1 - y_1^*}{y_1} \right) \frac{dy_1}{dt} + \frac{1}{c_5} \frac{dy_2}{dt}.$$

Using the equilibrium conditions at $E_3 = (x^*, y_1^*, 0)$ and simplifying (see Appendix D) yields

$$\frac{dV_3}{dt} \leq \left(b_3x^* + \alpha a b_2 c_4 k y_1^* + \alpha k_1 y_1^* - \frac{d_3}{c_5} \right) y_2 + \left(\frac{c_6}{c_5}k - \alpha k_1 - \frac{k_2}{c_5} \right) y_1 y_2.$$

Hence,

$$\frac{dV_3}{dt} < 0$$

provided that

$$b_3x^* + \alpha a b_2 c_4 k y_1^* + \alpha k_1 y_1^* < \frac{d_3}{c_5},$$

and

$$\frac{c_6}{c_5}k < \alpha k_1 + \frac{k_2}{c_5}.$$

Moreover,

$$\frac{dV_3}{dt} = 0$$

if and only if

$$(x, y_1, y_2) = (x^*, y_1^*, 0).$$

Therefore, by LaSalle's invariance principle, the equilibrium point $E_3 = (x^*, y_1^*, 0)$ is globally asymptotically stable. □

Biologically, these conditions indicate that the host predator persists together with the prey population when the kleptoparasitic predator fails to obtain sufficient benefit from kleptoparasitism interactions. Strong interspecific competition and limited kleptoparasitic gain may therefore drive the extinction of the second predator.

6. Numerical Simulation

In this section, we perform numerical simulations using the fourth-order Runge-Kutta (RK4) method in MATLAB to verify the analytical results and observe the global dynamics of system (2.1). We selected four distinct initial conditions to represent various ecological scenarios: $IC_1(3, 0.1, 2.5)$ for a kleptoparasite invasion, $IC_2(80, 1, 1)$ for prey abundance, $IC_3(2, 2.5, 0.5)$ for a state close to the equilibrium, and $IC_4(10, 5, 4)$ for predator overpopulation.

To maintain ecological realism, the energy conversion rate of kleptoparasitism (c_6) is not a static constant. It is coupled proportionally to the kleptoparasitism intensity (a), the host's predation rate (b_2), and the host's conversion efficiency (c_4). Assuming a transfer efficiency of 90%, we define $c_6 = 0.9(ab_2c_4)$. The fixed parameter values are as follows:

$$\begin{aligned} &r_1 = 0.75, \quad k = 100, \quad b_2 = 0.33, \quad b_3 = 0.3, \quad c_4 = 0.2, \quad c_5 = 0.3, \\ &k_1 = 0.1, \quad k_2 = 0.01, \quad d_2 = 0.1, \quad d_3 = 0.1, \quad \eta_1 = 0.005, \quad \eta_2 = 0.1. \end{aligned} \tag{6.1}$$

First, we evaluate the basic boundary equilibria. Based on Theorem 4.1, the predator-free state $E_1(100, 0, 0)$ is stable only if the carrying capacity k satisfies:

$$k < \frac{d_2}{b_2c_4 - \eta_1} = \frac{0.1}{0.33(0.2) - 0.005} \approx 1.6393.$$

Our carrying capacity is sufficiently large ($k = 100$). Because $100 > 1.6393$, the host predator overcomes natural mortality and prey defense, making E_1 always unstable. Next, Theorem 4.2 states that the kleptoparasite-only equilibrium E_2 requires $b_3c_5 > \eta_2$ to exist. In our setup, the prey defense is higher than the kleptoparasite's hunting efficiency ($0.09 < 0.1$). This makes x^* negative, meaning E_2 is biologically infeasible. Therefore, the subsequent numerical analysis focuses on the transitions between the kleptoparasite-exclusion state E_3 and the coexistence state.

6.1. The Impact of Kleptoparasitism Intensity.

We first analyze the effect of varying the kleptoparasitism intensity (a). At a low rate ($a = 0.3$, which yields $c_6 = 0.01782$), the system moves toward the boundary equilibrium:

$$E_3 = (1.639344, 2.235469, 0.0). \tag{6.2}$$

This indicates that the kleptoparasitic predator eventually dies out, leaving only the prey and the host predator.

We confirm its local stability using Theorem 4.3. With $b_2c_4 > \eta_1$ ($0.066 > 0.005$) and $b_3c_5 + c_6y_1^* > \eta_2$ ($0.1298 > 0.1$), the main stability condition gives:

$$\frac{k_2y_1^* + d_3}{b_3c_5 + c_6y_1^* - \eta_2} = \frac{0.01(2.235469) + 0.1}{0.3(0.3) + 0.01782(2.235469) - 0.1} \approx 4.1009. \tag{6.3}$$

Since $x^* = 1.639344 < 4.1009$, the requirement is completely satisfied, proving E_3 is locally asymptotically stable.

Figure 1 supports this analytical result. Trajectories from all four starting points converge to E_3. Ecologically, a 30% kleptoparasitism intensity is insufficient. The kleptoparasite cannot gather enough energy to survive the host's physical competition ($k_1 = 0.1$) and eventually starves.

We then raise the kleptoparasitism intensity to a moderate level ($a = 0.42$), yielding $c_6 \approx 0.02495$. The system undergoes a dynamic shift as a biologically valid coexistence state appears at:

$$E_4 = (9.442626, 0.861915, 1.315828).$$

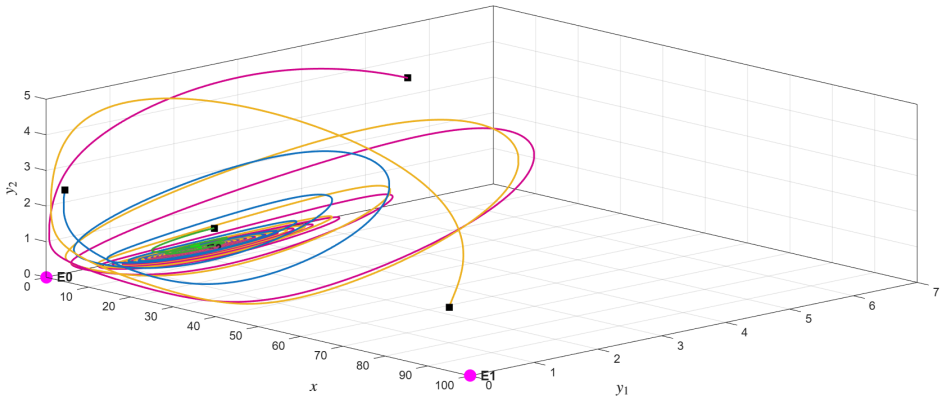

FIGURE 1. Phase portrait for $a = 0.3$ showing trajectory convergence to E_3.

Evaluating the Routh–Hurwitz criteria from Theorem 4.4 at E_4 gives:

$$\gamma_1 = 0.070820 > 0, \qquad \gamma_3 = 0.009622 > 0,$$

with a positive determinant condition:

$$\gamma_1\gamma_2 - \gamma_3 = 0.004633 > 0.$$

Since all conditions are met, E_4 is locally asymptotically stable.

Interestingly, based on Theorem 4.3, the boundary equilibrium E_3 also maintains its local stability here because the threshold condition ($x^* = 1.6393 < 2.6737$) remains satisfied. This indicates a phenomenon known as *bistability*, where the survival of the kleptoparasite is sensitive to the initial population sizes.

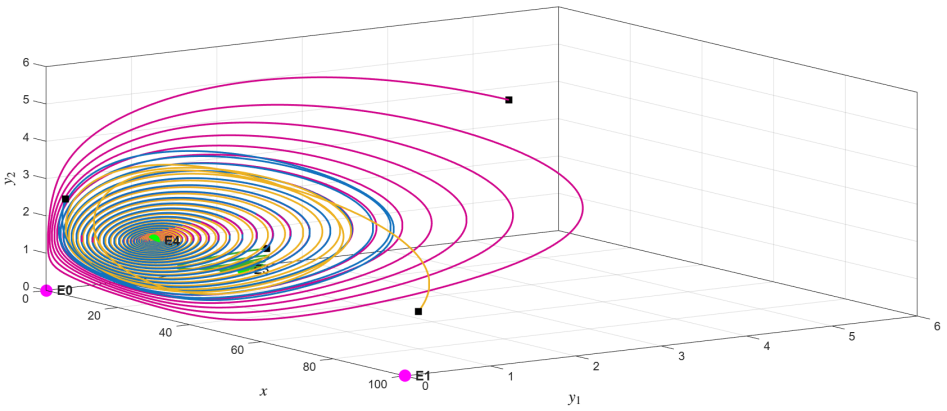

FIGURE 2. Phase portrait for $a = 0.42$ illustrating bistability between E_3 and E_4.

Figure 2 captures this bistability. Trajectories from IC_1, IC_2, and IC_4 spiral inward and settle at E_4. At a 42% kleptoparasitism intensity, the kleptoparasite obtains enough extra energy to survive alongside the other two species. Conversely, the trajectory from IC_3—where the host predator is already dominant—falls into the attraction basin of E_3. The host outcompetes the kleptoparasite before it can establish a stable population.

The dynamics become more complex when the kleptoparasitism intensity is further increased to $a = 0.5$ (yielding $c_6 = 0.0297$). The system exhibits the coexistence of attractors as the equilibrium shifts to:

$$E_4 = (18.774778, 0.525460, 1.452624).$$

Applying Theorem 4.4 gives:

$$\gamma_1 = 0.140811 > 0, \qquad \gamma_3 = 0.054030 > 0,$$

with a positive determinant:

$$\gamma_1\gamma_2 - \gamma_3 = 0.000770 > 0.$$

Mathematically, E_4 is locally asymptotically stable. The boundary equilibrium E_3 also stays stable ($x^* = 1.6393 < 2.0544$). However, numerical verification reveals that the basin of attraction for E_4 is extremely narrow.

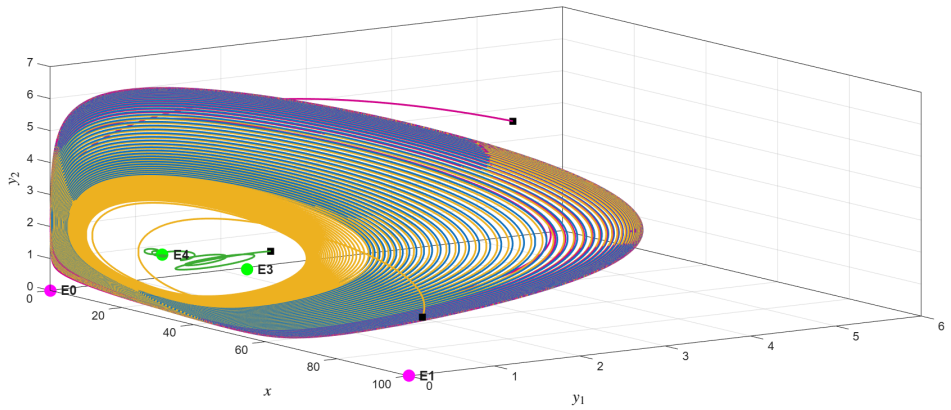

FIGURE 3. Phase portrait for $a = 0.5$ showing convergence to E_4 and sustained population oscillations.

Figure 3 illustrates the consequence of this weak attractive pull. The trajectory from IC_3 falls inside this narrow zone and slowly spirals into E_4. The other three initial conditions represent larger disturbances. Because E_4 is too weak to attract them, they exhibit sustained population oscillations.

Ecologically, a 50% kleptoparasitism intensity destabilizes the food web. Any significant fluctuation in population sizes will throw the system out of the stability basin, trapping all three species in continuous population oscillations.

Increasing the kleptoparasitism intensity to 80% ($a = 0.8, c_6 \approx 0.04752$) alters the system dynamics further. Evaluating the threshold condition from Theorem 4.3 reveals that E_3 loses its stability. The coexistence equilibrium moves to:

$$E_4 = (45.876377, 0.257489, 1.069852).$$

Checking Theorem 4.4 at this new location gives:

$$\gamma_1 = 0.344073 > 0, \qquad \gamma_3 = 0.532394 > 0,$$

and a clear positive determinant:

$$\gamma_1\gamma_2 - \gamma_3 = 0.003778 > 0.$$

As a result, E_4 regains robust stability, and the large-amplitude oscillations observed at $a = 0.5$ cease.

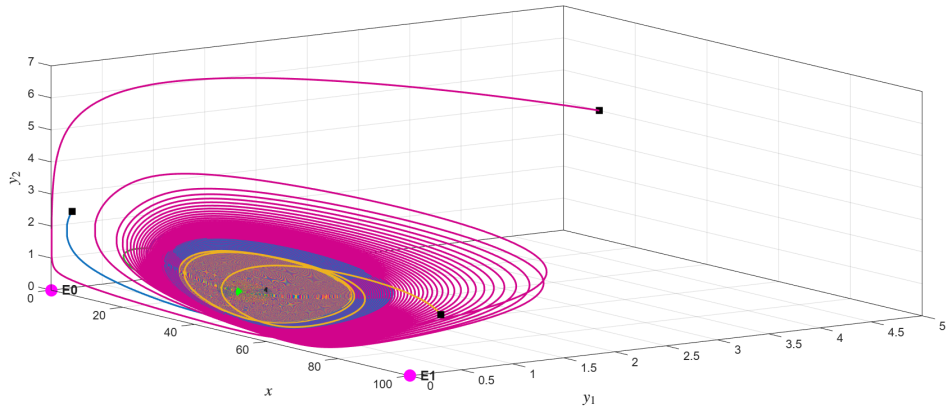

FIGURE 4. Phase portrait for $a = 0.8$ demonstrating damped oscillations converging to E_4.

As shown in Fig. 4, all four trajectories are forced toward E_4, characterized by slowly damping spirals. Although convergence is mathematically guaranteed, the system takes a prolonged time to stop oscillating before it settles.

In nature, this stabilization occurs because the host is significantly reduced. A kleptoparasitism intensity of 80% drops the host population to 0.257. With the host suppressed, the prey faces less predation pressure, and its population spikes to 45.876. Although the kleptoparasite steals a large proportion of food, its total population remains relatively low (1.069) because active hosts are scarce. This lack of hosts removes the energy required to sustain large oscillations, allowing the ecosystem to settle into a stable state.

6.2. **Bifurcation Analysis.** To observe the global behavior of the system over varying parameters, we construct one-dimensional bifurcation diagrams. We plot the local maximum and minimum values of the kleptoparasite population (y_2) using $IC_1(3, 0.1, 2.5)$. We selected this initial condition because it effectively captures the oscillatory behavior when the system becomes unstable.

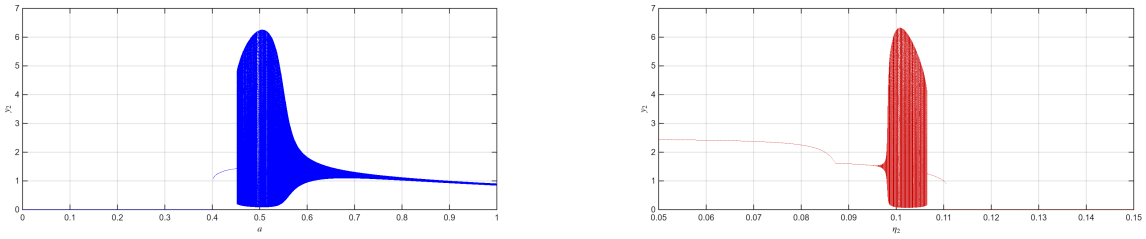

(A) Bifurcation with respect to a

(B) Bifurcation with respect to η_2

FIGURE 5. Extrema of the kleptoparasite population (y_2) with respect to a and η_2.

Figure 5(a) shows the dynamics of the system as the kleptoparasitism intensity (a) varies from 0 to 1. This result connects well with the prior phase portraits. When the kleptoparasitism intensity is low, the kleptoparasite population remains at zero, confirming the stability of E_3. As a increases, a single continuous line emerges, indicating stable coexistence. At intermediate values of a, the system loses stability and the populations oscillate continuously (represented by the thick blue area). Finally, when the kleptoparasitismintensity becomes extremely high, the oscillations cease, and the system returns to a stable state with a suppressed host population.

Next, we analyze the effect of prey defense (η_2) in Figure 5(b) with a fixed kleptoparasitism intensity of $a = 0.5$. The diagram identifies a limit near $\eta_2 = 0.09$. Below this threshold, the kleptoparasite hunts efficiently, keeping the ecosystem stable.

A major shift occurs when the prey defense exceeds 0.09. Independent hunting then requires more energy than the predator gains, forcing the kleptoparasite to rely mostly on stolen food. This dependency destabilizes the system and creates the large population oscillations shown by the dense red area. If the prey defense increases past 0.11, the stolen energy can no longer cover natural mortality, leading to total extinction.

To complete our numerical analysis, we combine the kleptoparasitism intensity (a) and prey defense (η_2) into a two-parameter ecological regime map in Figure 6. We classify the parameter space into three main regions based on the final state of the system: stable E_3 (gray), stable E_4 (green), and the oscillatory regime (blue).

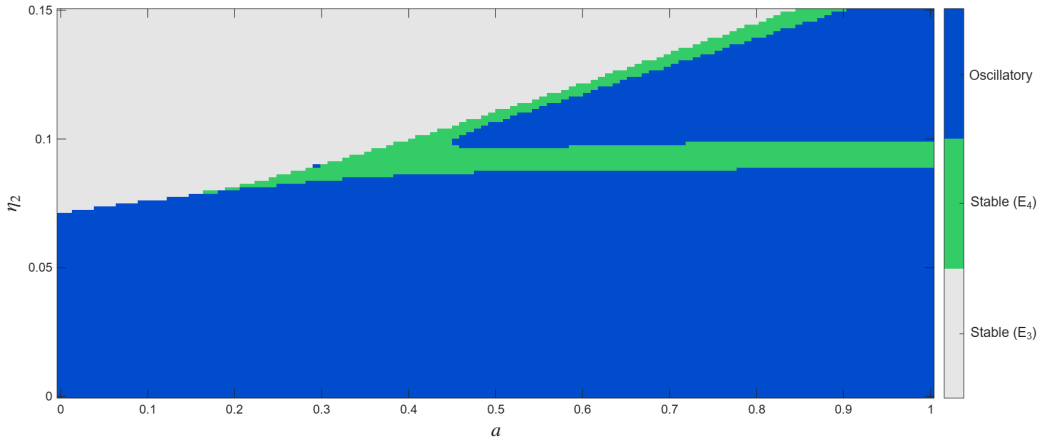

FIGURE 6. Two-parameter regime map in the (a, η_2)-plane: stable E_3 (gray), stable E_4 (green), and oscillatory dynamics (blue).

The gray region occupies the upper-left part of the map, where prey defense is strong and the kleptoparasitism intensity is low. The kleptoparasite cannot secure enough food and goes extinct. The upward slope of this boundary indicates that to survive a stronger prey defense, the kleptoparasite must steal more aggressively.

The blue region covers the entire lower section. When the prey defense is weak (below $\eta_2 \approx 0.08$), the predators hunt efficiently, leading to rapid population growth and subsequent declines, forming continuous cycles regardless of the kleptoparasitism intensity.

The green area indicates the narrow parameter space required for stable coexistence. At lower kleptoparasitism intensity, it forms a single diagonal line separating extinction from oscillation. However, for $a > 0.45$, this stable band splits into two branches.

The lower horizontal branch shows stability when the prey defense is moderate ($\eta_2 \approx 0.1$). The upper diagonal branch shows stability on the edge of extinction. A blue oscillatory wedge appears between these two green branches at high kleptoparasitism intensity. If the prey defense falls into this intermediate gap, the high kleptoparasitism intensity forces the ecosystem back into oscillations. This indicates that stable coexistence depends on a highly specific match between prey defense and kleptoparasitic behavior.

7. Discussion and Conclusion

This study proposes and analyzes a three-dimensional predator–prey model that incorporates a biomass-transfer formulation for kleptoparasitic behavior and active prey defense. The well-posedness of the system is established through the existence, positivity, and boundedness of solutions. Local and global stability analyses are carried out to determine the threshold conditions governing the extinction, persistence, and coexistence of the interacting populations.

The analytical and numerical results indicate that the kleptoparasitism intensity (a) and prey defense (η_2) play key roles in shaping the qualitative dynamics of the ecosystem. Under a low kleptoparasitism intensity, the kleptoparasitic predator fails to secure sufficient energy and faces extinction. A moderate increase in the kleptoparasitism intensity allows for stable coexistence. In this regime, numerical simulations show that the system exhibits bistability, indicating that the survival of the kleptoparasite is sensitive to the initial population sizes. As the kleptoparasitism intensity increases further, the local attraction of the coexistence state weakens. Under these conditions, the system loses its stable coexistence and begins to exhibit sustained population oscillations. Conversely, a very high kleptoparasitism intensity significantly suppresses the host predator population, which dampens the oscillations and allows the system to settle into a stable equilibrium.

Furthermore, numerical exploration of the parameter space suggests an ecological trade-off between the prey and the kleptoparasite. As the prey defense strengthens, the kleptoparasite requires a higher kleptoparasitism intensity to avoid extinction. However, the parameter region supporting stable coexistence remains narrow. If the species interaction falls outside this balance, the system destabilizes into continuous population oscillations. This indicates that stable coexistence in this kleptoparasitic food web depends on a specific balance between prey evasion and predator kleptoparasitism.

Several extensions of the present model can be considered for future work. Time delays could be incorporated to represent delayed predator responses or the maturation time of prey defense mechanisms. More general functional responses, such as Holling type-II or type-III forms, may also provide additional ecological realism. Finally, a rigorous analytical study on the emergence of Hopf bifurcations and the calculation of the first Lyapunov coefficients would provide a complete mathematical characterization of the oscillatory boundaries observed numerically in this study.

Appendix A. Derivation of the Coexistence Equilibrium

This appendix derives the coexistence equilibrium

$$E_4 = (x^*, y_1^*, y_2^*).$$

Setting

$$\frac{dx}{dt} = \frac{dy_1}{dt} = \frac{dy_2}{dt} = 0,$$

system (2.1) becomes

$$r_1 x\left(1 - \frac{x}{k}\right) - b_2 x y_1 - b_3 x y_2 = 0,$$

$$b_2 c_4 x y_1 - a b_2 c_4 x y_1 y_2 - k_1 y_1 y_2 - d_2 y_1 - \eta_1 x y_1 = 0,$$

$$b_3 c_5 x y_2 - k_2 y_1 y_2 - d_3 y_2 + c_6 x y_1 y_2 - \eta_2 x y_2 = 0.$$

For the coexistence equilibrium, we assume

$$x > 0, \qquad y_1 > 0, \qquad y_2 > 0.$$

From the second equilibrium equation, we obtain

$$x^* = \frac{k_1 y_2^* + d_2}{b_2 c_4 - a b_2 c_4 y_2^* - \eta_1}.$$

Similarly, the third equilibrium equation gives

$$y_1^* = \frac{d_3(b_2 c_4 - a b_2 c_4 y_2^* - \eta_1) - (b_3 c_5 - \eta_2)(k_1 y_2^* + d_2)}{c_6(k_1 y_2^* + d_2) - k_2(b_2 c_4 - a b_2 c_4 y_2^* - \eta_1)}.$$

Substituting these expressions into the first equilibrium equation yields the cubic polynomial

$$c_3 y_2^3 + c_2 y_2^2 + c_1 y_2 + c_0 = 0,$$

where

$$\begin{aligned}
c_3 =& k_1 k a b_2 b_3 c_4 c_6 + k k_2 a^2 b_2^2 b_3 c_4^2,\\
c_2 =& k k_1 a b_2^2 c_4 \eta_2 - k d_3 a^2 b_2^3 c_4^2 - k k_1 a b_2^2 b_3 c_4 c_5 - k_1 r_1 k a b_2 c_4 c_6\\
&- k k_2 a^2 r_1 b_2^2 c_4^2 - k_1^2 r_1 c_6 - k_1 k_2 a r_1 b_2 c_4 + k k_1 \eta_1 b_3 c_6\\
&- k k_1 b_2 b_3 c_4 c_6 - 2 k k_2 a b_2^2 b_3 c_4^2 + 2 k k_2 a \eta_1 b_2 b_3 c_4\\
&+ k a b_2 b_3 c_4 c_6 d_2,\\
c_1 =& k k_1 r_1 b_2 c_4 c_6 + 2 k k_2 a r_1 b_2^2 c_4^2 - k k_1 \eta_1 r_1 c_6 - 2 k k_2 a \eta_1 r_1 b_2 c_4\\
&- k_2 a d_2 r_1 b_2 c_4 - 2 r_1 c_6 k_1 d_2 - k a r_1 b_2 c_4 c_6 d_2 + k_1 k_2 r_1 b_2 c_4\\
&- k_1 k_2 \eta_1 r_1 + 2 d_3 k a b_2^3 c_4^2 - 2 d_3 k a \eta_1 b_2^2 c_4\\
&- k a b_2^2 b_3 c_4 c_5 d_2 + k a b_2^2 c_4 \eta_2 d_2 - k k_1 b_2^2 c_4 \eta_2\\
&+ k k_1 b_2^2 b_3 c_4 c_5 + k k_1 \eta_1 \eta_2 b_2 - k k_1 \eta_1 b_2 b_3 c_5\\
&+ k k_2 b_2^2 b_3 c_4^2 - k b_2 b_3 c_4 c_6 d_2 - 2 k k_2 \eta_1 b_2 b_3 c_4\\
&+ k \eta_1 b_3 c_6 d_2 + k k_2 \eta_1^2 b_3,\\
c_0 =& k r_1 b_2 c_4 c_6 d_2 - k k_2 r_1 b_2^2 c_4^2 + 2 k k_2 \eta_1 r_1 b_2 c_4 - k \eta_1 r_1 c_6 d_2\\
&- k k_2 \eta_1^2 r_1 - r_1 c_6 d_2^2 + k_2 d_2 r_1 b_2 c_4 - k_2 d_2 \eta_1 r_1\\
&+ 2 d_3 k \eta_1 b_2^2 c_4 - d_3 k b_2^3 c_4^2 - d_3 k \eta_1^2 b_2\\
&+ k d_2 b_2^2 b_3 c_4 c_5 - k d_2 \eta_1 b_2 b_3 c_5 - k d_2 \eta_2 b_2^2 c_4\\
&+ k d_2 \eta_1 \eta_2 b_2.
\end{aligned}$$

The positive real root of this cubic polynomial determines y_2^* and consequently the coexistence equilibrium E_4.

Appendix B. Derivation of the Lyapunov Function for E_1

For the predator-free equilibrium point $E_1 = (k, 0, 0)$, consider the Lyapunov function

$$V_1(x, y_1, y_2) = x - k - k \ln \frac{x}{k} + y_1 + y_2.$$

Differentiating V_1 along the trajectories of system (2.1) gives

$$\frac{dV_1}{dt} = \left(\frac{x-k}{x}\right)\frac{dx}{dt} + \frac{dy_1}{dt} + \frac{dy_2}{dt}.$$

Substituting system (2.1), we obtain

$$\begin{aligned}
\frac{dV_1}{dt} =& (x-k)\left[r_1\left(1 - \frac{x}{k}\right) - b_2 y_1 - b_3 y_2\right] + b_2 c_4 x y_1 - a b_2 c_4 x y_1 y_2 - k_1 y_1 y_2\\
&- d_2 y_1 - \eta_1 x y_1 + b_3 c_5 x y_2 - k_2 y_1 y_2 - d_3 y_2 + c_6 x y_1 y_2 - \eta_2 x y_2.
\end{aligned}$$

Using the identity

$$(x-k)\left(1-\frac{x}{k}\right)=-\frac{(x-k)^2}{k},$$

it follows that

$$\begin{aligned}\frac{dV_1}{dt}=&-\frac{r_1}{k}(x-k)^2-(x-k)(b_2y_1+b_3y_2)+b_2c_4xy_1-ab_2c_4xy_1y_2-k_1y_1y_2\\&-d_2y_1-\eta_1xy_1+b_3c_5xy_2-k_2y_1y_2-d_3y_2+c_6xy_1y_2-\eta_2xy_2.\end{aligned}$$

Since all solutions are bounded and $x\le k$, we have

$$-(x-k)(b_2y_1+b_3y_2)\le kb_2y_1+kb_3y_2.$$

Moreover,

$$-ab_2c_4xy_1y_2\le 0,\qquad -\eta_1xy_1\le 0,\qquad -\eta_2xy_2\le 0.$$

Therefore,

$$\begin{aligned}\frac{dV_1}{dt}\le&kb_2y_1+kb_3y_2+b_2c_4xy_1-k_1y_1y_2-d_2y_1\\&+b_3c_5xy_2-k_2y_1y_2-d_3y_2+c_6xy_1y_2.\end{aligned}$$

Using the boundedness condition $x\le k$, we further obtain

$$b_2c_4xy_1\le b_2c_4ky_1;\qquad b_3c_5xy_2\le b_3c_5ky_2;\qquad c_6xy_1y_2\le c_6ky_1y_2.$$

Hence,

$$\frac{dV_1}{dt}\le\left[kb_2(1+c_4)-d_2\right]y_1+\left[kb_3(1+c_5)-d_3\right]y_2+\left[c_6k-k_1-k_2\right]y_1y_2.$$

Appendix C. Derivation of the Lyapunov Function for E_2

For the equilibrium point

$$E_2=(x^*,0,y_2^*),$$

consider the Lyapunov function

$$V_2(x,y_1,y_2)=x-x^*-x^*\ln\frac{x}{x^*}+\frac{1}{c_4}y_1+\alpha\left(y_2-y_2^*-y_2^*\ln\frac{y_2}{y_2^*}\right),$$

where

$$\alpha=\frac{b_3}{b_3c_5-\eta_2}>0.$$

Differentiating V_2 along the trajectories of system (2.1) gives

$$\frac{dV_2}{dt}=\left(\frac{x-x^*}{x}\right)\frac{dx}{dt}+\frac{1}{c_4}\frac{dy_1}{dt}+\alpha\left(\frac{y_2-y_2^*}{y_2}\right)\frac{dy_2}{dt}.$$

Substituting system (2.1), we obtain

$$\begin{aligned}\frac{dV_2}{dt}=&(x-x^*)\left[r_1\left(1-\frac{x}{k}\right)-b_2y_1-b_3y_2\right]\\&+\frac{1}{c_4}\left[b_2c_4xy_1-ab_2c_4xy_1y_2-k_1y_1y_2-d_2y_1-\eta_1xy_1\right]\\&+\alpha(y_2-y_2^*)\left[(b_3c_5-\eta_2)x-k_2y_1-d_3+c_6xy_1\right].\end{aligned}$$

Using the equilibrium relations

$$1-\frac{x^*}{k}=\frac{b_3y_2^*}{r_1},\qquad d_3=(b_3c_5-\eta_2)x^*,$$

together with

$$x=x^*+(x-x^*),$$

yields

$$\begin{aligned}\frac{dV_2}{dt} =& -\frac{r_1}{k}(x-x^*)^2 - b_2(x-x^*)y_1 - b_3(x-x^*)(y_2-y_2^*)\\ &+\frac{1}{c_4}\left[b_2c_4xy_1 - ab_2c_4xy_1y_2 - k_1y_1y_2 - d_2y_1 - \eta_1xy_1\right]\\ &+b_3(x-x^*)(y_2-y_2^*) - \alpha k_2y_1(y_2-y_2^*) + \alpha c_6xy_1(y_2-y_2^*).\end{aligned}$$

After cancellation and using the bound

$$x \le k,$$

we obtain

$$\frac{dV_2}{dt} \le \left(b_2x^* + \alpha k_2y_2^* - \frac{d_2}{c_4}\right)y_1 + \left(\alpha c_6k - \frac{k_1}{c_4} - \alpha k_2\right)y_1y_2.$$

Appendix D. Derivation of the Lyapunov Function for E_3

For the equilibrium point

$$E_3 = (x^*, y_1^*, 0),$$

consider the Lyapunov function

$$V_3(x,y_1,y_2) = x - x^* - x^*\ln\frac{x}{x^*} + \alpha\left(y_1 - y_1^* - y_1^*\ln\frac{y_1}{y_1^*}\right) + \frac{1}{c_5}y_2,$$

where

$$\alpha = \frac{b_2}{b_2c_4 - \eta_1} > 0.$$

Differentiating V_3 along the trajectories of system (2.1) gives

$$\frac{dV_3}{dt} = \left(\frac{x-x^*}{x}\right)\frac{dx}{dt} + \alpha\left(\frac{y_1-y_1^*}{y_1}\right)\frac{dy_1}{dt} + \frac{1}{c_5}\frac{dy_2}{dt}.$$

Substituting system (2.1), we obtain

$$\begin{aligned}\frac{dV_3}{dt} =&(x-x^*)\left[r_1\left(1-\frac{x}{k}\right) - b_2y_1 - b_3y_2\right]\\ &+\alpha(y_1-y_1^*)\left[(b_2c_4-\eta_1)x - ab_2c_4xy_2 - k_1y_2 - d_2\right]\\ &+\frac{1}{c_5}\left[b_3c_5xy_2 - k_2y_1y_2 - d_3y_2 + c_6xy_1y_2 - \eta_2xy_2\right].\end{aligned}$$

Using the equilibrium relations

$$1 - \frac{x^*}{k} = \frac{b_2y_1^*}{r_1}, \qquad d_2 = (b_2c_4 - \eta_1)x^*,$$

together with

$$x = x^* + (x - x^*),$$

yields

$$\begin{aligned}\frac{dV_3}{dt} =& -\frac{r_1}{k}(x-x^*)^2 - b_2(x-x^*)(y_1-y_1^*) - b_3y_2(x-x^*)\\ &+b_2(x-x^*)(y_1-y_1^*) - \alpha ab_2c_4xy_2(y_1-y_1^*) - \alpha k_1y_2(y_1-y_1^*)\\ &+\frac{1}{c_5}\left[b_3c_5xy_2 - k_2y_1y_2 - d_3y_2 + c_6xy_1y_2 - \eta_2xy_2\right].\end{aligned}$$

After cancellation and using the bound

$$x \le k,$$

we obtain

$$\frac{dV_3}{dt} \le \left(b_3x^* + \alpha ab_2c_4ky_1^* + \alpha k_1y_1^* - \frac{d_3}{c_5}\right)y_2 + \left(\frac{c_6}{c_5}k - \alpha k_1 - \frac{k_2}{c_5}\right)y_1y_2.$$

Competing interests. The author declares no competing interests.

REFERENCES

[1] A.J. Lotka, Elements of Physical Biology, Williams and Wilkins, Baltimore, 1925.

[2] V. Volterra, Fluctuations in the Abundance of a Species Considered Mathematically, Nature 118 (1926), 558–560. https://doi.org/10.1038/118558a0.

[3] A. Suryanto, I. Darti, Dynamics of Leslie-Gower Pest-Predator Model with Disease in Pest Including Pest-Harvesting and Optimal Implementation of Pesticide, Int. J. Math. Math. Sci. 2019 (2019), 5079171. https://doi.org/10.1155/2019/5079171.

[4] K. Pusawidjayanti, A. Suryanto, R.B.E. Wibowo, Dynamics of a Predator-Prey Model Incorporating Prey Refuge, Predator Infection and Harvesting, Appl. Math. Sci. 9 (2015), 3751–3760. https://doi.org/10.12988/ams.2015.54340.

[5] H.M. Ulfa, A. Suryanto, I. Darti, Dynamics of Leslie-Gower Predator-Prey Model with Additional Food for Predators, Int. J. Pure Appl. Math. 115 (2017), 199–209. https://doi.org/10.12732/ijpam.v115i2.1.

[6] R. Resmawan, A. Suryanto, I. Darti, H.S. Panigoro, A Dynamical Analysis of a Predator-Prey Model: Exploring the Influence of the Allee Effect, Environmental Protection, and Supplementary Food Sources, Jambura J. Biomath. 6 (2025), 311–328. https://doi.org/10.37905/jjbm.v6i4.32685.

[7] D. Das, P. Bora, S. Mondal, S. Borah, P. Gogoi, An Analysis of a Two Predator One Prey Model with Predator Advantage, J. Pharm. Negat. Results 13 (2022), 1679–1689.

[8] R. Babu, P. Gayathri, Mathematical Study of One Prey and Two Competing Predators Considering Beddington-DeAngelis Functional Response with Distributed Delay, Hilbert J. Math. Anal. 2 (2023), 1–19. https://doi.org/10.62918/hjma.v2i1.14.

[9] N.H. Aljahdaly, Theoretical and Semi-Analytical Simulation for a Two-Predator-One-Prey Model during the Mating Period, PLoS One 18 (2023), e0289410. https://doi.org/10.1371/journal.pone.0289410.

[10] E.V. Iyengar, Kleptoparasitic Interactions throughout the Animal Kingdom and a Re-evaluation, Based on Participant Mobility, of the Conditions Promoting the Evolution of Kleptoparasitism, Biol. J. Linn. Soc. 93 (2008), 745–762. https://doi.org/10.1111/j.1095-8312.2008.00954.x.

[11] R.D. Holt, G.A. Polis, A Theoretical Framework for Intraguild Predation, Am. Nat. 149 (1997), 745–764. https://doi.org/10.1086/286018.

[12] S. Focardi, M. Materassi, G. Innocenti, D. Berzi, Kleptoparasitism and Scavenging Can Stabilize Ecosystem Dynamics, Am. Nat. 190 (2017), 398–409. https://doi.org/10.1086/692798.

[13] X. Wang, L. Zanette, X. Zou, Modelling the Fear Effect in Predator–Prey Interactions, J. Math. Biol. 73 (2016), 1179–1204. https://doi.org/10.1007/s00285-016-0989-1.

[14] A. Batabyal, Predator–Prey Systems as Models for Integrative Research in Biology: the Value of a Non-Consumptive Effects Framework, J. Exp. Biol. 226 (2023), jeb245851. https://doi.org/10.1242/jeb.245851.

[15] D. Mukherjee, Stability and Bifurcation of a Two Competing Prey-One Predator System with Anti-Predator Behavior, Jambura J. Biomath. 3 (2022), 1–11. https://doi.org/10.34312/jjbm.v3i1.13820.

[16] Z.Kh. Alabacy, A.A. Majeed, The Local Bifurcation Analysis of Two Preys Stage-Structured Predator Model with Anti-Predator Behavior, J. Phys. Conf. Ser. 2322 (2022), 012061. https://doi.org/10.1088/1742-6596/2322/1/012061.

[17] C. Zhang, S. Liu, J. Huang, W. Wang, Stability and Hopf Bifurcation in an Eco-Epidemiological System with the Cost of Anti-Predator Behaviors, Math. Biosci. Eng. 20 (2023), 8146–8161. https://doi.org/10.3934/mbe.2023354.

[18] Q. Din, R.A. Naseem, M.S. Shabbir, Predator–Prey Interaction with Fear Effects: Stability, Bifurcation and Two-Parameter Analysis Incorporating Complex and Fractal Behavior, Fractal Fract. 8 (2024), 221. https://doi.org/10.3390/fractalfract8040221.

[19] M. Yang, C. Xiang, Y. Yang, Spatiotemporal Patterns in a Predator–Prey Model with Anti-Predation Behavior and Fear Effect, Adv. Contin. Discrete Models 2025 (2025), 26. https://doi.org/10.1186/s13662-025-03881-4.

[20] D. Bhattacharjee, D. Das, S. Acharjee, T.K. Dutta, Two Predators, One Prey Model That Integrates the Effect of Supplementary Food Resources Due to One Predator's Kleptoparasitism under the Possibility of Retribution by the Other Predator, Heliyon 10 (2024), e28940. https://doi.org/10.1016/j.heliyon.2024.e28940.

[21] D. Anggreini, A. Suryanto, I. Darti, W.M. Kusumawinahyu, M.A.J.D. Putra, Nonlinear Dynamics of a Predator-Prey System with Kleptoparasitic Interactions, Commun. Math. Biol. Neurosci. 2026 (2026), 77. https://doi.org/10.28919/cmbn/9967.

[22] T.A. Putri, D. Savitri, Analysis of Predator-Prey Dynamics Using Holling Type I & II Response Functions with Kleptoparasitism and Anti-Predator Behavior, Jambura J. Biomath. 7 (2026), 42–59. https://doi.org/10.37905/jjbm.v7i1.8.